Nanoscale

Accepted Manuscript

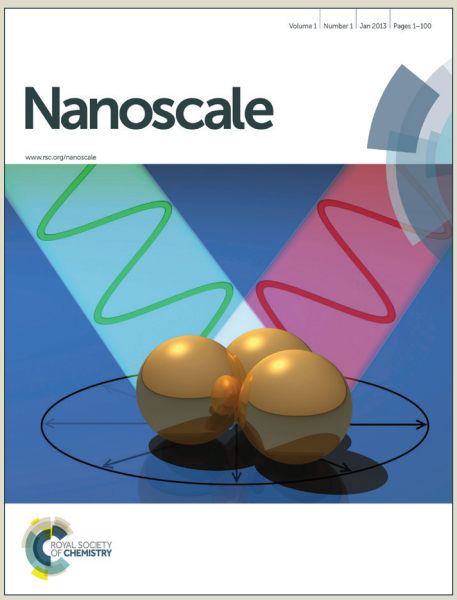

ROYAL SOCIETY OF CHEMISTRY

www.rsc.org/nanoscale

Nanoscale

ARTICLE

Hydrophobic pocket targeting probe for enteroviruses †

Mari Martikainen[a,d], *Kirsi Salorinne*[b,d], *Tanja Lahtinen*[b,d], *Sami Malola*[c,d], *Perttu Permi*[a,b,d,e], *Hannu Häkkinen*[b,c,d*] *and Varpu Marjomäki*[a,d*]

Received 00th January 20xx,
Accepted 00th January 20xx

DOI: 10.1039/x0xx00000x

www.rsc.org/

Visualization and tracking of viruses without compromising their functionality is crucial in order to understand virus targeting to cells and tissues, and to understand the subsequent subcellular steps leading to virus uncoating and replication. Enteroviruses are important human pathogens causing a vast number of acute infections, and are also suggested to contribute to the development of chronic diseases like type I diabetes. Here, we demonstrate a novel method to target site-specifically the hydrophobic pocket of enteroviruses. A probe, a derivative of Pleconaril was developed and conjugated to various labels that enabled visualization of enteroviruses in light and electron microscopy. The probe mildly stabilized the virus particle by increasing the melting temperature by 1-3 degrees, and caused a delay in the uncoating of the virus in cellular endosomes, but could not however inhibit the receptor binding, cellular entry or infectivity of the virus. The hydrophobic pocket binding moiety of the probe was shown to bind to echovirus 1 particle by STD and tr-NOESY NMR methods. Furthermore, binding to echovirus 1 and coxsackievirus A9, and to a lesser extent to coxsackievirus B3 was verified by gold nanocluster labeled probe by TEM analysis. Molecular modelling suggested that the probe fits the hydrophobic pockets of EV1 and CVA9, but not of CVB3 as expected, correlating well with the variations in the infectivity and stability of the virus particles. EV1 conjugated to fluorescent dye labeled probe was efficiently internalized to the cells. The virus-fluorescent probe conjugate accumulated in the cytoplasmic endosomes and caused infection starting from 6 hours onwards. Remarkably, before and during the time of replication, the fluorescent probe was seen to leak from the virus-positive endosomes and thus separate from the capsid proteins that were left in the endosomes. These results suggest that, like the physiological hydrophobic content, the probe may be released upon virus uncoating. Our results collectively thus show that the gold and fluorescently labeled probes may be used to track and visualize the studied enteroviruses during early phases of infection opening new avenues to follow virus uncoating in cells.

Introduction

Enterovirus genus belongs to the family of *Picornaviridae* containing numerous clinically important human pathogens and causing a variety of diseases from common cold and mild rash to viral meningitis and paralysis.[1] Some viruses, especially in the coxsackie group, have been associated also with chronic diseases such as type 1 diabetes.[2] Moreover, members of enteroviruses, like human enterovirus 71, have recently been causing serious acute infections and great threat to public health.[3]

Enteroviruses have an icosahedron shaped protein capsid consisting of 60 copies of each of the structural proteins (VPs 1 to 4). The non-enveloped capsid encloses the 7.5-kb-long single-stranded positive-sense RNA genome. VP1 proteins surround the five-fold axis while VP2 and VP3 alternate around the two- and three-fold axes, while VP4 is a shorter internal protein.[4] Within the capsid protein VP1, there is a hydrophobic pocket which is occupied by a pocket factor (natural lipid) of each virus.[5] The pocket entrance is located at the end of the canyon-like depression surrounding the five-fold axis. The pocket factors have been anticipated to play a role in the capsid stability since their expulsion seems to be needed for the genome release.[6–8] Replacement of the pocket factor with a compound having much higher binding affinity could be an efficient antiviral tool acting on the virus capsid. This has been demonstrated with viruses whose receptor binding occurs in the canyon region of the capsid, triggering the uncoating process.[6,9]

Although enteroviruses have a huge impact on human health, their pathogenicity is not fully understood. Still, little is known about the subcellular structures that mediate infection of non-enveloped enteroviruses. In recent applications, detection of the virus from tissues and cells is usually based on indirect antibody labelling methods e.g. immunofluorescence, immunohistochemistry and electron microscopic methods. In addition, the nucleic acid of the infectious virus can be detected with specific probes coupled with *in situ*-hybridization and different PCR methods.[13] However, all these

[a] *Department of Biological and Environmental Science, University of Jyväskylä, FI-40014 Jyväskylä, Finland; Email: varpu.s.marjomaki@jyu.fi; Tel: +358-40-5634422*
[b] *Departmen of Chemistry University of Jyväskylä, FI-40014 Jyväskylä, Finland; Email: hannu.j.hakkinen@jyu.fi; Tel +358-400-247973*
[c] *Departmen of Physics, University of Jyväskylä, FI-40014 Jyväskylä, Finland*
[d] *Nanoscience Center, University of Jyväskylä, FI-40014 Jyväskylä, Finland*
[e] *Institute of Biotechnology, University of Helsinki, FI-00014 Helsinki, Finland.*
† Electronic Supplementary Information (ESI) available: [Details of the synthesis of the probes, UV Vis absorption spectra of probe (**2**), PAGE separation and the absorption spectra of the gold labeled probe (**3**), details of the NMR experiments, determination of the cytotoxicity of the studied molecules, TEM micrographs of the gold labeled probe (**3**) with enteroviruses, live cell imaging of the fluorescent probe (**4**) in cells, and additional details of modeling of the hydrophobic pockets.]. See DOI: 10.1039/x0xx00000x

methods bring challenges in terms of background and sensitivity.[14,15] Novel, covalently bound probes are needed to facilitate live experiments in animals or visualizing specific domains for high-resolution microscopy. We previously demonstrated the production and specificity of a cysteine targeted gold cluster probe against enteroviruses. [16]

None of the indirect labeling methods or stable covalent probes mentioned above are able to bring crucial dynamic information about virus uncoating inside cellular structures – the key event leading to successful infection in cells and tissues. Our understanding on the actual site of virus uncoating comes from recent structural studies of purified enteroviruses, such as polio and coxsackievirus A7 (CVA7)[17], revealing that the actual site of capsid opening is at the 2-fold axis. These and other studies also suggest that enteroviruses are differently sensitive to receptor interactions. For poliovirus, receptor binding starts the uncoating process, whereas for both coxsackievirus A9 (CVA9) and echovirus 1 (EV1), receptor binding stabilizes the virus structure.[18] Thus the capsid opening for many enteroviruses must rely on cellular cues that trigger the virus opening after virus entry to the cytoplasmic endosomes. Therefore, it is important to have reliable techniques to follow the uncoating of the virus *in vivo* and *in vitro* in order to elucidate the cellular factors leading to the release of their genome.

Presently there are no direct tools to follow virus uncoating by microscopy in cells and animal models. Despite its supposedly important role for virus uncoating, there is no understanding of the mechanistic role of the hydrophobic pocket for this process. This is mainly due to the fact that no probes are presently available to follow the function of the hydrophobic pocket. **Pleconaril, one of the designated WIN compounds, is one of the most studied capsid binding inhibitors.[10–12] However, the efficacy of Pleconaril as an inhibitor is not exceedingly high for many enteroviruses suggesting that slight modifications of the molecule could provide a more dynamic imaging tool for binding without compromising viral infectivity.**

Here, we created a novel dynamic probe to enable virus labeling through the hydrophobic pocket both for live fluorescent imaging, as well as, for ultrastructural studies. We show that the probe does bind to selected members of the enterovirus B group, which get mildly stabilized due to binding, and can be followed through the early steps of virus infection.

Materials and methods

Cells and viruses. Viruses EV1 (Farouk strain) and CVB3 (Nancy strain) were obtained from the American Type Culture (ATCC) and CVA9 (Griggs strain). All viruses were propagated in the GMK cells (ATCC) and purified in a 10 to 40% sucrose gradient as described earlier.[19,20] Infectivity of purified virus was determined by TCID50 assay, and the purity and RNA and protein content were determined by spectroscopic analysis and protein measurement using the Zlotnik method.

The human lung carcinoma A549 cell line was obtained from ATCC and they were maintained in Dulbecco's modified Eagle's medium (DMEM) containing 10% fetal bovine serum (FBS) supplemented with penicillin and streptomycin (P/S) and Glutamax. The green monkey kidney (GMK) cells were obtained from ATCC and maintained in Minimum Essential Medium Eagle containing 10% FBS and P/S and Glutamax.

CPE-inhibition- and TCID50/ml assay. The cytopathic effect (CPE)-inhibitory assays were performed using an overall scheme similar to that described earlier.[21] To summarize, the experiments were carried out using 2-day-old A549 cell (8 x 10^4 cells/well) in 96-well cell culture plates. The cell culture media was changed to fresh DMEM (1% FBS). Cells were infected with MOI 5 and the amount of virus was kept constant on each well. Viruses were pre-incubated for 1 h at 37°C with the studied compounds before the assay. For CPE-assay, 100 µM concentrations of the studied compounds were used during pre-incubation with the virus, and then diluted ten-fold when added on cells. For 50% inhibitory concentration (IC_{50}) quantifications the compounds were tested in various concentrations from 0.6 to 200 µM in 2-fold dilutions. IC_{50} value for gold probe **(3)** was quantified using concentrations from 0.2 to 14 µM, and for fluorescent probe **(4)** from 3.5 to 500 µM. Infected cells without the test compounds and non-infected cells served as virus only control (vc) and cell control (cc), respectively. After 24 h infection, crystal violet formalin solution was used to fix and stain the cells. The dye was extracted and optical density was quantified spectrophotometrically at 570 nm with Victor™ X4 2030 Multilabel Reader (Perkin Elmer). CPE values were calculated using the following equation: $\%\,\mathrm{CPE} = 100 - ([[\mathrm{ODvirus} + \mathrm{compound} - \mathrm{ODvc}] / \mathrm{ODcc}]\ \mathrm{x}\ 100)$. Virus only controls were set to 100 % CPE and cells only to 0 %, respectively. The IC_{50} values were calculated by regression analysis.

The 50% tissue culture infective dose ($TCID_{50}$) was calculated as previously described.[22] Briefly, the GMK cells were grown on 96-well plates to subconfluency. Viruses were pre-incubated for 1 h at 37°C with the studied compounds before the assay. After the pre-incubation samples were added to the first wells and then serially diluted using 1 log dilutions. After 72 h of incubation, the cells were stained using crystal violet formalin solution for 10 min at room temperature. Detached cells were washed off with water and the remaining cells were counted as viable and non-infected. The $TCID_{50}$/ml values were calculated by using the Reed-Muench formula.

PaSTRy assay. The thermostability of purified EV1, CVA9 and CVB3 was evaluated by Particle Stability Thermal Release Assay performed as previously described.[23] Briefly, reactions were carried out in a thin-walled PCR plates (Agilent) containing 1 µg of EV1, CVA9 or CVB3, 100 µM of the probe (2), -derivative (1) or Pleconaril and 10 x SYBR Green II (Invitrogen) in PBS, pH = 7.4. Viruses were pre-incubated for 1 h at 37°C with the studied compounds before the thermostability assay. The release of viral genome was detected with the SYBR Green II dye in a Bio-Rad C1000 thermal cycler by raising the temperature gradually from 20°C to 90°C, with fluorescence recorded in quadruple at 0.5°C intervals. The Bio-Rad CFX

manager 2.1 software was used to define the melting temperature (T_m) of each sample. In detail, the T_m was measured from the inflection point (dI/dT) of the fluorescence intensity (I) as functions of temperature (T) from the derivative plot.

Immunofluorescence labelling and confocal microscopy. For immunofluorescence assay a saturative amount (500 µM, 50 000 x molar excess of the ligand over the hydrophobic pocket) of fluorescent probe **(4)** was first bound to 12.9 µg amount of EV1 for 1 h at 37°C in 2 mM $MgCl_2$ PBS. Unbound dye was dialyzed three times against 500 ml of PBS supplemented with 2 mM $MgCl_2$ using 50,000-molecular-mass-cutoff Spectra/Por Micro Float-A-Lyzer cellulose ester membranes (Spectrum Laboratories). For the cell experiments A549 cells were grown on coverslips to subconfluency. EV1-fluorescent probe conjugate was first bound to the cells for 1 h on ice in DMEM (1% FBS), after which the cells were washed and with PBS, and after incubation at 37°C (in 1% DMEM) they were fixed at RT with 4% paraformaldehyde (PFA) for 30 min. Fixed samples were permeabilized with 0.2% Triton X-100 for 5 min, and labeled with polyclonal rabbit antiserum against EV1 (produced as described in[24]) and anti-rabbit secondary antibody Alexa Fluor 488 (Invitrogen). The cells were mounted to ProLong Gold antifade reagent 4′-6-diamidino-2-phenylindole (Invitrogen) and examined with an Olympus microscope IX81 with a Fluo-View-1000 confocal setup.

In addition, a live imaging experiment was performed in which A549 cells were infected similarly as described above with the EV1-fluorescence probe conjugate. Cells were imaged at different time points (30 min, 4 h, 12 h and 24 h) before fixation. Finally cells were fixed, permeabilized and labeled as described above.

TEM. The binding of gold probe **(3)** to different viruses' hydrophobic pockets was visualized with transmission electron microscope (TEM) JEM-1400 (JEOL). First 14 µM of gold probe **(3)** was incubated with 12.9 µg of virus for 1 h at 37°C in PBS. In addition, high-molecular weight EV1-gold conjugate was separated from the small unconjugated gold using a 1 ml Sephacryl (Sephacryl S-300 high resolution, GE Healthcare) column according to manufacturer´s instructions. The Butvar-coated copper grids were glow discharged (EMS/SC7620 mini-sputter coater), and samples were added on the grids for 15 s. After which the excess sample was blotted away with a blotting paper (Whatman 3MM). Virions were visualized by gentle negative staining with 1% (wt/vol) phosphotungstic acid (PTA). Stain was added for 30 s, excess dye blotted away as before. Samples were air dried overnight and imaged with TEM.

Results

Probe design, structure and synthesis

"WIN compounds" – named after the developer Sterling-Winthrop – are a family of antiviral drugs designed to target the early events (attachment, entry and uncoating) of viral replication (Scheme 1).[2,11,25] WIN compounds have been shown to bind specifically into the interior hydrophobic pocket located at the VP1 protein of enterovirus capsid replacing the naturally occurring lipid.[26–29] Therefore, the WIN framework, which is best known for Pleconaril (WIN 63843), was chosen as the basis for the design of a probe that would target the hydrophobic pocket of the virus capsid and bind via non-covalent interactions. **Our previous data (unpublished) on the best known WIN compound Pleconaril (WIN 63843), however, showed only a minor effect on EV1 infectivity despite the suspected binding ability to the hydrophobic pocket of the virus. Therefore, Pleconaril was chosen for further modification to develop a probe that would label the hydrophobic pocket with good enough affinity, but without compromising the infectivity of the virus.**

The WIN framework in its simplicity consists of two rigid aromatic planar ring systems of isoxazole (unit A) and phenyl-oxadiazole (unit B) that are connected by a flexible propyloxy unit (Scheme 1). Based on earlier studies[10,11,25,28] the phenyl-oxadiazole ring system binds to the deeper end of the viral hydrophobic pocket and, consequently, the isoxazole ring located at the open end of the pocket was therefore chosen as the site for a linker unit that would reach out to the surface of the virus particle. This was accomplished by incorporating a carboxylic acid functionality at the 3-position of the isoxazole ring, to which a C-11 alkyl chain with a terminal hydroxyl group was then attached via an amide linkage (Scheme 2). Here, the amide group was also intended as an anchoring group that would hold the probe in place in the hydrophobic pocket. The optimal length provided by the C11-alkyl chain was determined by molecular modeling to be long enough for the linker unit to reach out from the mouth of the hydrophobic pocket to the viral capsid surface. Hydroxyl group at the end to the linker arm provided further linking to gold clusters or fluorescent dye labels via an ester bond formation (Scheme 2).

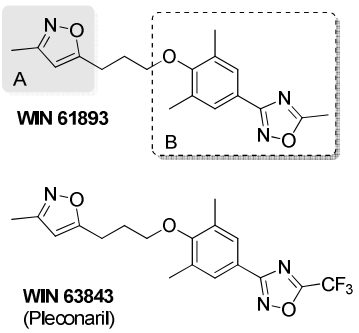

Scheme 1. Molecular structures of two representatives WIN compounds highlighting the different structural units A and B.

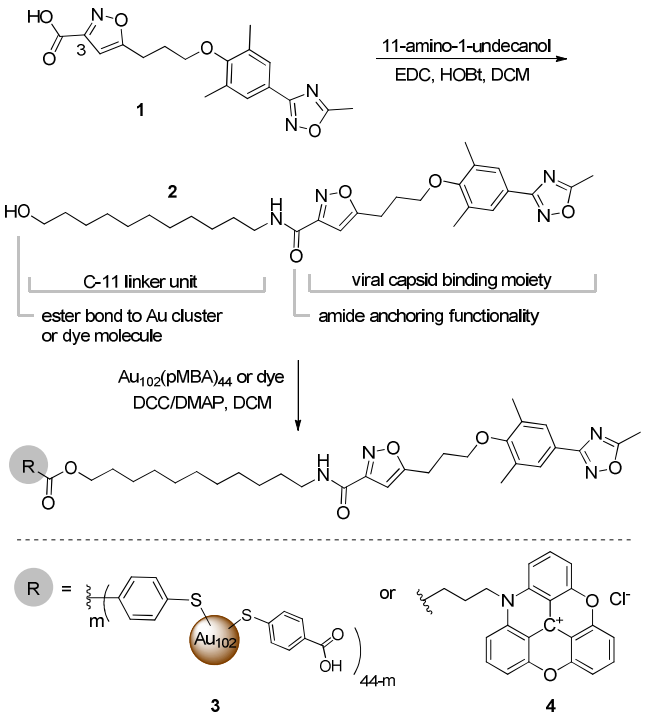

Scheme 2. Synthesis and molecular structures of the probes **(2)**, and the gold **(3)** and dye **(4)** labels of the probe. C11-linker unit, viral capsid binding moiety, amide anchoring functionality and terminal hydroxyl group for further reactions with gold clusters or dye molecules via ester bond formation are highlighted. EDC = N-(3-dimethylaminopropyl)-N′-ethylcarbodiimide, HOBt = 1-hydroxybenzotriazole, DCC = dicyclocarbodiimide, DMAP = N,N-dimethylaminopyridine and DCM = dichloromethane.

Synthesis of the probe **(2)** was accomplished by an amide coupling reaction of the carboxylic acid derivative[30] **(1)** with 11-amino-1-undecanol in dichloromethane in the presence of N-(3-dimethylaminopropyl)-N′-ethylcarbodiimide (EDC) coupling reagent and a catalytic amount of 1-hydroxybenzotriazole (HOBt) in good yield (Scheme 2). Subsequent Stieglich esterification reaction with p-mercaptobenzoic acid (pMBA) protected $Au_{102}(pMBA)_{44}$ cluster[31,32] or azadioxatriangulenium dye molecule[33,34] in DCM in the presence of dicyclohexylcarbodiimide (DCC) and a catalytic amount of N,N-dimethylaminopyridine (DMAP) afforded the gold **(3)** and fluorescent dye **(4)** labeled probes (see SI for details).

Probe does not compromise the infectivity of enteroviruses

As the produced probes were based on an antiviral molecule that was however slightly modified, we wanted to study the toxicity of the probe **(2)** and derivative **(1)** to cells and whether they affected virus infectivity. All the assays were also done with Pleconaril for comparison. First, we studied the effects of each derivative and Pleconaril on cell viability without the virus. A 3-(4,5-dimethylthiazol-2-yl)-2,5-diphenyltetrazolium bromide (MTT) assay verified that the studied compounds or Pleconaril did not cause any significant cell death (Figure S5D).

In order to test the effects of derivative **(1)**, probe **(2)**, gold probe **(3)**, fluorescent probe **(4)** and Pleconaril on virus infectivity we applied several well characterized approaches. Firstly, we used the TCID50 assay in which 50 % tissue culture infective dose is quantified with and without the studied compounds. In this assay, the infection is followed to the end (end-point-dilution) so that the assay reveals the last dilution, which still contains infective particles. In the assay, the TCID50 value is finally calculated from the dilutions. Strikingly, the assay revealed that the infectivity of the virus with the studied compounds was not affected (Figure 1A & Figure S5). The infectivity was typically in the order of 1010 to 1011 TCID50/ml.

Next we studied the effect of the compounds with a shorter time scale, with a 24 h cytopathic effect (CPE) inhibition assay, which is also an established method to evaluate virus infectivity.[21] In this method the antiviral effect of the compound is quantified using a crystal violet uptake of the live cells. The quantification is performed with an optical plate reader and the cell viability is calculated from the optical reading values. This assay verified that there was a delay in infection rather than total inhibition of the infection (Figure 1B): after 24 h, probe **(2)** inhibited infection of EV1 by 65 %, that of CVA9 by 67 % and that of CVB3 by 18 %. Pleconaril seemed to have the strongest inhibitory effect on all viruses, whereas the studied derivatives showed a smaller effect at these earlier time points suggesting that the modification and derivatization of the Pleconaril core changed the activity only slightly. In addition, with CPE assay we quantified the half maximal inhibitory concentrations (IC_{50} (μM)) for each compound (Figure S5A). All the compounds showed the least effect on CVB3 as expected, since previously Pleconaril has been shown not to fit the Nancy strain of CVB3.[10] Consequently the IC_{50} values of for CVB3 were a considerably higher than for EV1 or CVA9. This assay is based on a 24 h time point, which is why it differs from the end-point-titration result and shows more similarity with the CPE result that similarly relies on a 24 h time point. Thus the IC_{50} measurement is not as reliable as a method to compare the real inhibitory effects between the different compounds used.

As the total number of infective particles revealed by end-point-dilution was not changed in the preparations with the probe **(2)**, we wanted to study this delay in more detail with additional assays. Namely, confocal microscope immunofluorescence studies were performed to evaluate the kinetics of the infective pathways (Figure 1C). We performed the infection by first binding the viruses on ice, then washing the unbound viruses at 0°C before allowing the virus enter the cell at 37°C. This ensured the entry of the viruses in the cells via receptor binding and not by fluid phase uptake of the virus. First of all, there were no apparent differences in the amount of virus internalized to cells with or without the probe suggesting that it did not interfere with receptor binding. The infected cells were evaluated after different time periods of 6 h, 12 h and 24 h post infection (p.i.). After these periods, cells were fixed and labeled using antibodies against the major capsid proteins. This allowed us to visualize the viruses first in

cytoplasmic endosomes, and then, typically after 3 h or more, the massive production of new capsid proteins in the cytoplasm was seen as a widespread cytoplasmic stain that verified the start of replication. This way we were able to count the number of infected cells after various time periods and treatments. This capsid labeling may show the number of infected cells more sensitively than previously described CPE assay. The analysis clearly revealed that the start of infection was delayed: normally, the number of infected cells increased quickly after 4 to 6 h p.i. Now, in the presence of probe **(2)** or derivative **(1)** the same number of infected cells as in the control infection after 12 h was observed after 24 h with EV1 or CVA9. Thus, virus treated with the probe seemed to stay longer in the endosomes and produced new viral proteins with a slower pace, but was still as infective as the native virus. All methods described above showed an effect with EV1 and CVA9 but not with CVB3.

We also used another different method to measure cell viability after various time points with native viruses or viruses treated with studied compounds. This method is based on measuring ATP levels of cells. This measurement verified the results that were revealed by the more conventional infectivity tests: after short period of incubation with cells, the studied compounds slowed down the CPE, but, after longer time periods, the viability was lost also with viruses treated with the same compounds (Figure S6).

Probe increases mildly the stability of the viruses

One of the effects of antiviral drugs, and especially that of the drugs targeting to the hydrophobic pocket, has been suggested to act via stabilization of the hydrophobic pocket.[35] If the drug molecule replaces the fatty acid in the hydrophobic pocket and remains there longer period of time, it could stabilize the virus particle by not allowing the dynamic changes to occur in the active areas during the uncoating event of the virus. This would also be seen as an increase in the stability upon warming the virus particles to non-physiologial high temperatures.

Therefore, we studied the thermal stability of virus capsids with Particle Stability Thermal Release Assay (PaSTRy), where release of viral RNA is promoted with gradual heating and detected with SYBR Green II dye. PaSTRy is developed to investigate the dynamics of viral uncoating and viral stability.[23] We studied the stabilizing effects of compounds **(1)** and **(2)** using always Pleconaril as a comparison. The melting temperature (T_m) at which purified virus releases its genome was determined for each virus (Figure 2). These were 50.5°C, 50°C and 44.5°C for EV1, CVA9 and CVB3, respectively. CVB3 was the most unstable during the heating as it showed remarkable 5 degree difference to the other enteroviruses. The PaSTRy assay showed an increase in the stability of the viruses treated with derivative **(1)**, by increasing 2.5 and 4 degrees of the melting temperature for EV1 and CVA9, respectively. For CVB3 derivative **(1)** had a negligible change in the melting temperature, yet, probe **(2)** showed only little effect on the thermal stability of all the studied viruses.

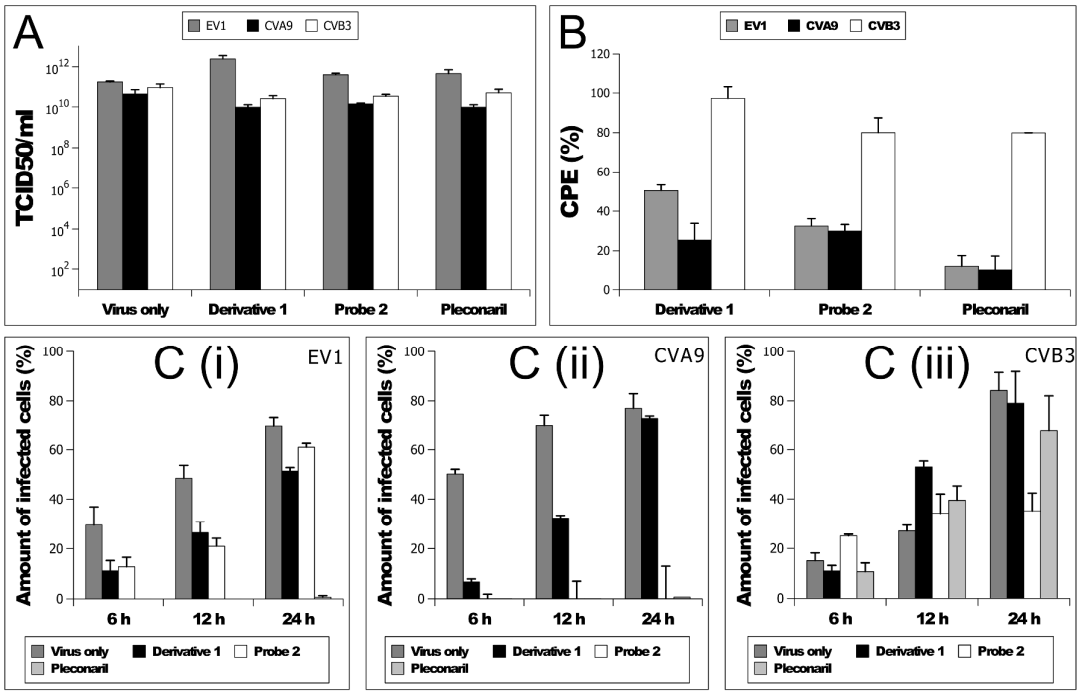

Figure 1: Effects on virus infectivity. The concentration of studied compounds was 100 µM in all experiments. A) Amount of infective particles ($TCID_{50}$/ml) was calculated with end-point titration assay. Experiment was performed three times, and the means are shown (± standard errors (SE)). B) Effects to short term infectivity were studied with 24 h CPE inhibition assay. In B the controls containing virus only the values were set to 100 % CPE and with cells only to 0 %. The results are shown as mean values from three different independent experiments (± SE). C) The inhibiting effect was studied further on EV1 (i), CVA9 (ii) and CVB3 (iii) by quantifying the amount of infected cells at different time points.

A

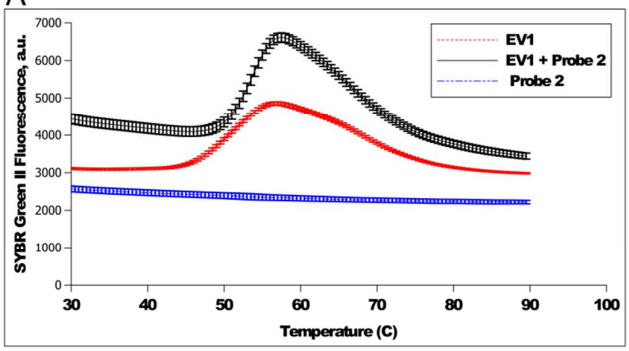

B

Tm (°C)	Virus only	Probe 2	Derivative 1	Pleconaril
EV1	50.5 (± 0.33)	53.5 (± 0.14)	55.0 (± 0.13)	56.0 (± 0.00)
CVA9	50.0 (± 0.14)	51.0 (± 0.14)	55.0 (± 0.00)	55.5 (± 0.00)
CVB3	44.5 (± 0.14)	44.5 (± 0.00)	44.5 (± 0.00)	47.5 (± 0.00)

Figure 2. PaSTRY assay of EV1, CVA9 and CVB3 with derivative **(1)**, probe **(2)** and Pleconaril. A) Fluorescence curves of EV1 with and without the probe **(2).** Release of the RNA is detected as SYBR Green II Fluorescence. B) Tm of all viruses and compounds (± SE from four independent experiments).

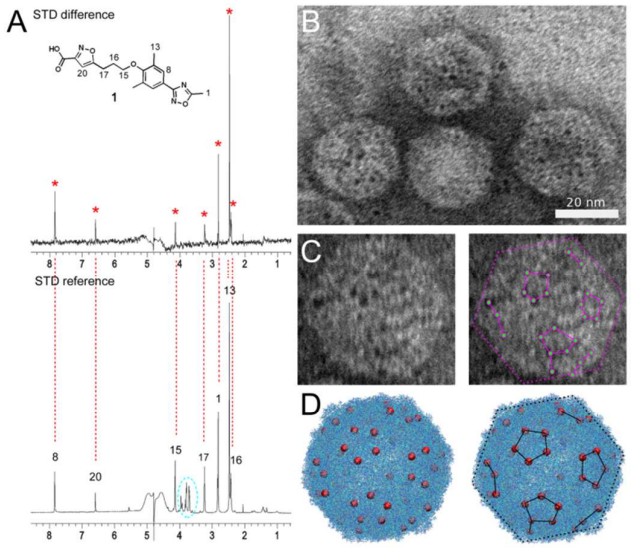

Figure 3. Binding of the probe into the hydrophobic pocket**.** A) STD NMR experiment of EV1 virus particle and derivative **(1)** in D_2O at 37°C: The upper STD spectrum showing the signals of derivative **(1)** as a result to binding to EV1 (red asterisk) and the lower reference spectrum (with off-resonance irradiation only) of EV1 and derivative **(1)**. Chemical shifts marked with cyan color are impurities in the virus sample. In B) and C) are shown TEM images of column purified EV1-gold probe conjugates. In D) is shown a model structure of EV1 with red spheres denoting the positions of the hydrophobic pocket entrances. Orientation of the model structure is arranged to agree with the experimentally observed shape of the virus and the positions of gold probe **(3)** that are drawn in purple and in black.

Probe binds to enteroviruses

In order to study the binding of the probe into the enterovirus hydrophobic pocket in solution, saturation transfer difference (STD)[36] NMR studies were performed. Due to the poor solubility of probe **(2)** in aqueous solution, derivative **(1)** was used instead as a model compound to simulate the viral capsid binding moiety of the probe. A 5000-fold excess of derivative **(1)** over the hydrophobic binding sites of EV1 virus particle in 2 mM $MgCl_2$-PBS buffer in D_2O was used to record the STD NMR spectra with 1 – 3.5 s saturation times. The STD difference spectra showed distinct signals belonging to derivative **(1)**, which indicated binding to EV1 virus particle (Figure 3A). Similar binding was also observed with a complementary transfer NOESY experiment, furthermore demonstrating the successful binding of derivative **(1)** to EV1 virus capsid in aqueous solution (Figure S4).

The requirement and basis of an STD NMR experiment relies on weak binding of the ligand to the virus particle.[37,38] Therefore, due to the rapid exchange between the bound and the free ligand, magnetization from the virus particle is transferred to the bound ligand and can only be detected when the bound ligand is released back to solution. Hence, the STD NMR measurement both gives evidence of the derivative **(1)** binding to the virus particle, as well as, demonstrates the dynamic nature of the binding process.

Gold cluster- and fluorescent dye conjugates bind to virus capsids

The binding of gold cluster probe **(3)** to virus capsid was monitored by TEM (Figure 3B-C, S7). The probe **(3)** was mixed with purified viruses in PBS containing 2 mM $MgCl_2$ at 37°C to allow conjugation to the virus particles. We used 1 h incubation to evaluate the extent of binding. The gold-virus conjugate was added on a TEM grid with or without negative staining and the binding was monitored directly in a microscope. TEM revealed that gold cluster probes bound to EV1 and CVA9 capsids forming pentamer-like symmetries (Figure 3B-C, S7A-B). The gold probes **(3)** usually occupied only a small fraction of the total 60 hydrophobic pockets. In order to remove the excess gold from the preparations, we used Sephacryl S-300 column purification based on size exclusion. After the column purification we could still see similar binding of scattered gold clusters to EV1 virus confirming that binding of the gold probes **(3)** to virus was strong enough to withstand short elution of the virus conjugate preparation with buffer. TEM analysis of CVB3 (Figure S7C) did not show similar kind of binding in pentamer-like symmetries than EV1 and CVA9, as expected.

In addition to TEM analysis, we studied whether the addition of gold cluster probe **(3)** had any effect on the infectivity of the viruses. Similar to what was observed with compounds **(1)** and **(2)**, gold probe **(3)** delayed the infection rather than inhibit it altogether (Figure S5C). There was no difference in the number of infected virus particles based on end-point-titration assay (Figure S5B).

Additionally, we used fluorescent probe **(4)** in order to follow the enteroviruses in cells (Figure 4A). Conjugation of the fluorescent probe **(4)** to the virus particles was done similarly than described above with the gold probe **(3)**. The fluorescent probe-virus mixture was extensively dialyzed before adding on cells in order to avoid loosely bound fluorescent probe **(4)** with viruses. In addition, we fixed the cells and labeled the virus with antibodies against capsid proteins in order to follow the virus with another method as well in case the dye would come off the virus at some point. The antibody labeling of the viruses verified that virus was indeed present in the virus-fluorescent probe conjugate and no loose dye was entering the endosomes. Also, separate control experiments with the fluorescent probe **(4)** without the virus verified that the dye did not accumulate in endosomes without the virus (Figure S8). During the first hours of virus entry to cells, virus capsid label and fluorescent probe **(4)** was only present in cytoplasmic vesicles colocalizing well together, as expected.

We have shown before that EV1 and CVA9 capsids stay in the endosomes, whereas typically at 3 h p.i. and later, virus replication is observed as the resulting high cytoplasmic accumulation of newly made capsid proteins.[39,40] For both native viruses and virus-fluorescent probe conjugates, the number of infected cells increased rapidly after 6, 12 and 24 h. However, as was observed with the other infectivity methods, virus-fluorescent probe conjugates stayed a longer time in the vesicles before the start of replication. The quantitation of the infected cells after different time points showed that virus-fluorescent dye conjugates showed always 30 % less infected cells at every time point (Figure 4B).

The fluorescent probe **(4)** comes off the virus by dissociating most probably due to an opening of the virus (Figure 4C). This is a gradual process, happens in endosomes as the virus capsids themselves do not leak from the endosomes to the cytoplasm. Thus, the dissociated fluorescent probe **(4)** is first located inside endosomes, and then leaks through the endosomal membrane as time passes**.** Even though the leaking from the endosomes starts from 6 h onwards, these are the real rate limiting steps in the viral infection, and the possible delay in the uncoating and/or release will greatly postpone the outcome of the infection. Release of the viral genome from the endosomes is one important rate limiting step in enterovirus infection, and any delay in uncoating may lower the probability

Live imaging of the fluorescent probe **(4)** conjugated to EV1 in cells showed high values of the fluorescent probe in endosomes, but clearly lower amounts after longer incubation times suggesting that a separation of the dye from the virus had occurred (Figure S9). The loose dye was observed in the cytoplasm nearby the endosomes after 6 and 8 h but the level of the fluorescent signal was already very faint after 12 to 24 h (Figure S10). This further demonstrates the dynamic nature of the fluorescent probe **(4)** binding.

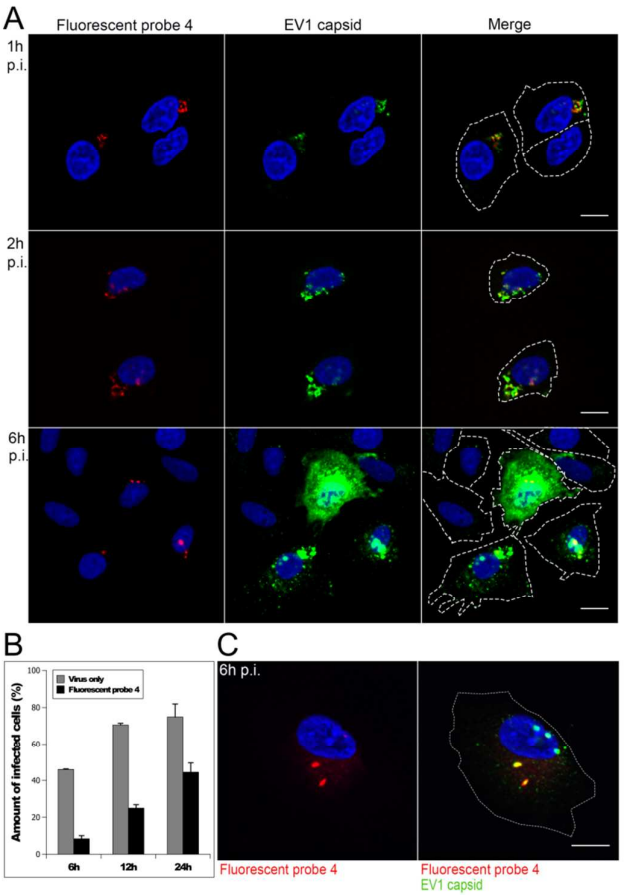

Figure 4. Fluorescent probe **(4)** conjugated to EV1 and internalized into cells. A) The internalization of the virus-fluorescent probe conjugate was followed from 1 h to 6 h. Fluorescent probe **(4)** was seen in the same vesicular structures than EV1 capsid label (green). Scale bars 10 µm. B) The amount of infected cells was calculated at different time points p.i. from confocal microscope images. C) Fluorescent probe **(4)** leaked from the endosomes to cell cytoplasm after 6 h of infection. Scale bar 10 µm.

Modeling of the hydrophobic pocket

In order to understand the differences between the interactions of probe **(2)** with EV1, CVA9 and CVB3 we examined the structures of their hydrophobic pockets and analyzed the solvent accessible volumes using their crystal structures[4,18,41] (for details of the analysis method, see the Supporting Information text). The overall structure of the pocket and arrangement of the surrounding protein chains in EV1 and CVA9 are similar while that of CVB3 is different (Figure 5). There is a direct “main entrance” into the pocket in all of the three viruses and in addition a narrower “side entrance”. The main entrance into the pocket is the most open in EV1 with an opening of at least 6 Å for the whole pocket (Figure. S11). Thus, there is enough space for the probe **(2)** to enter into the pocket in full. For CVA9 there is a narrow 1Å gap in the main entrance at the center of the pocket (Figure. S11B), but otherwise the surface is well open and the pocket large enough for the probe, especially if the dynamic effects of

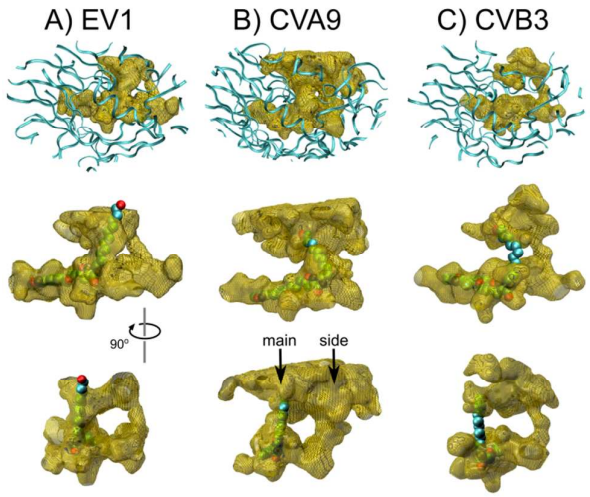

Figure 5. Space-filling models of the hydrophobic pocket with the nearby protein chains shown (top panels), with probe **(2)** inserted inside for EV1, CVA9 and CVB3 (center and bottom panels). The center and bottom illustrations show the same pocket with about 90 degree rotation.

the capsid might open the small closure in the way in. Most importantly, the direct entrance to the pocket in CVB3 is significantly more closed at the center of the pocket.

The structure of the side entrance is also favoring EV1, and especially CVA9, in possible binding of probe molecules (Figure 5A, B). First, the average width of the side route is the narrowest in CVB3 for all of the three viruses (Figure 5C). Second, the side entrance is the farthest from the actual pocket in CVB3 as compared to EV1 and CVA9. Both of these factors indicate that replacing of the fatty acid and binding of the probe in CVB3 are more difficult than in EV1 and CVA9. By looking at the general structure of the pocket, the binding properties of the probe molecules on EV1 and CVA9 are expected to be very similar. Analyzing the binding properties of EV1 and CVA9 more closely reveals that the aromatic rings of the probe **(2)** molecule have reasonably good possibilities to bind to the pocket in both viruses, but the possibilities for anchoring the amide functional group (shown in Scheme 2) into the bottom of the main entrance are much better in CVA9 compared to EV1. The minor static structural differences in the dimensions of the entrances of EV1 and CVA9 are most probably becoming negligible as the dynamics of the virus capsids is taken into account.

Discussion

We have developed a novel probe targeting the hydrophobic pockets of selected enteroviruses **but without compromising the infectivity of the virus.** As far as we know, this is the first study to specifically label and visualize the pocket by using both gold nanoclusters and fluorescent dye as visualizing tags. Probes that have been recently designed for enteroviruses have been suggested to act as antiviral agents[3,10,29,42] However, probes that replace the natural hydrophobic moiety, but do not compromise the infectivity and uncoating of the virus, could also act as potential markers and tools to study the function of the hydrophobic pocket.

The probe developed here is a derivative of Pleconaril, which was originally designed to fit the pocket and stabilize the capsid and thus act as an antiviral.[12] The results observed here with the new derivatives of Pleconaril suggest that the derivatization has probably changed the binding ability of the modified Pleconaril moiety as they all showed a very similar change on virus infection compared to original Pleconaril: A delayed infection but no lowering of the final infectivity. Pleconaril was first designed against rhinoviruses, for which it shows a good inhibitory effect on virus replication, but also several other enteroviruses, such as CVB1, CVB5, and CVA9 have been shown to be sensitive to Pleconaril.[10] Since then, several modifications of Pleconaril have been designed showing varying antiviral effects, and thus suggesting variations in the pocket structure.[43] Here, derivative **(1)** was synthesized by modifying the structure of WIN 61893 to 1) provide a link to gold clusters or fluorescent dye, and to 2) provide an anchoring group that would hold the probe in place at the open end of the hydrophobic pocket via hydrogen bonding. The stability of the virus-conjugations to gold clusters and fluorescent dye was verified by column purification of the unbound gold and extensive dialysis of the unbound dye.

In our study we tested three different enteroviruses belonging to the same HEV B subgroup of enteroviruses, namely EV1, CVA9 and CVB3 Nancy strain. Pleconaril was already earlier shown not to fit into the hydrophobic pocket of the Nancy strain of CVB3 due to amino acid substitutions of Ile1092 to Leu or Ile1092 to Met.[10,43] This was also observed as high IC_{50} values in *in vitro*-studies and as low protective efficacy in mouse models.[10] CVB3 Nancy thus acted as a good negative control in our study, as it did not show good binding of the gold probe **(3)** to this virus in TEM. In concordance with this, our probes **(1** & **2)** based on Pleconaril could not change the melting temperature of the Nancy strain.

TEM results of EV1 and CVA9 suggested that only some of the 60 possible hydrophobic pockets may be replaced by our probe at any given time. Presently, there is no information on how well the hydrophobic pockets are occupied by fatty acids. The most thorough study was performed on bovine enterovirus with mass spectrometry of the fatty acids found in the virus structure.[6] That study showed some variation in the repertoire of the used fatty acids, the palmitic acid being the most used fatty acid suggesting that it is the best length for the pocket structure. Yet, there is no direct information about if all the pockets are normally occupied by fatty acids and if all of them or only some pockets close to the uncoating site are emptied during uncoating. There is a consensus in the field that the occupancy of the pockets by the pocket factors has a definite role in capsid stabilization.[6,8,44] Without no direct proof and only a few tools to study the pocket factors, the function and significance of the pocket has remained elusive so far.

Importantly, our TEM results suggested that some exchange between our probe and the natural fatty acid in the

pocket might occur, as this exchange did not lead to an empty virus. However, whether the sites that more easily exchange the fatty acid to our probe are close to the hotspot of the uncoating, remains to be studied. Another alternative is of course that some pockets are naturally empty and our probe would fit those empty sites more easily. The studies that we performed using STD and trNOESY NMR gave more understanding on the dynamic nature of the binding and release of the pocket factor. Namely, the NMR methods used in this study are based on dynamic binding and release of the probe from the virus. That is the only way the virus may magnetize the small probe that is then measured after release from the hydrophobic pocket in the experiment. The NMR results thus indicate that there is most likely indeed some dynamic exchange of the pocket factor in the hydrophobic pocket. Previously, the binding of another Pleconaril derivative was also studied with this same method by Benie et al.[36] However, the specific binding of the tested drug, REPLA 394, to the hydrophobic pockets of the virus capsid was demonstrated using a competition STD titration experiments with a more potent viral inhibitor (WIN 52084). Here, in our study, we were able to directly see the magnetization of the probe and could thus confirm its binding to the virus. Since the testing of all derivatives by STD NMR was impossible due to solubility issues, it is possible that some differences might occur in the binding affinity. However, considering the very similar behavior of all derivatives in their effects on infectivity, those differences may remain small.

The dynamic binding and release of the pocket factor may be one result of capsid breathing. Capsid breathing has been studied with different picornaviruses, e.g. for poliovirus,[45] HRV14, HRV16[7,46], swine vesicular disease virus[47] and CVA9. In addition, breathing has been detected with other ssRNA viruses such as some of the noda-[48] and tetraviruses[49]. It was shown for HRV14 by cryo EM, and further explored by MD simulation, that during the breathing procedure VP4 and N-terminus of VP1 extrude the capsid temporarily.[7] Similarly, cryo EM reconstruction of the poliovirus (PV1) has shown VP1 outside the capsid for the native virus close to the 2-fold axis where the uncoating has been shown to occur.[45] Thus, the capsid breathing is an important part of the virus dynamics and under specific circumstances may lead to uncoating process of the virus, and further, to virus replication.[9,26,50] The capsid binding inhibitors have been shown to stabilize the virus particles. Mechanistically this may occur by decreasing the breathing of the virus capsid, which has been verified by mass spectroscopy (MC-MS and MALDI-MS).[26,50]

The stability of the enterovirus structure is reflected in its melting temperature. This method has been used more recently also for virus capsid binding probes.[3,51,52] While the extent of increase is difficult to extrapolate directly to the real inhibition of infection, it is a convenient way to monitor the effects of drugs to the viruses and compare the viruses to each other. The new (four 3-(4-pyridyl)-2-imidazolidinonen derivatives) capsid inhibitor molecules were shown to increase the melting temperature of EV71 by 2-4 degrees and that of EVD68 with Pleconaril by 4 degrees.[3,51] This increase with EV71, however, was preceded by a lengthy 24 h to 72 h incubation with a high amount of inhibitor used (200 μM). For native enteroviruses the melting temperature vary between 44.5 and 58 degrees.[3] The foot and mouth disease virus has been shown to be more thermolabile.[53] This may be due to the lack of hydrophobic pocket altogether in FMDV, and argues for the importance of the pocket factor in enteroviruses. The enteroviruses are very robust viruses and can stand long time at room temperature or repeated freeze-thaw cycles without losing infectivity (data not shown). We observed with our probes that they increased the stability of the studied enteroviruses by increasing the melting temperature by 1 to 4.5 degrees (Figure 4). However, this only delayed the infection cycle of EV1 and CVA9 roughly by 12 and 24 h, respectively, but did not inhibit the infection (Figure 1).

Changes in the infectivity upon antiviral treatment have been studied using various methods, which make it difficult to compare the results between different studies. Scmidtke et al.[21] established a high-throughput CPE inhibitory assay for CVB3, influenza A virus and herpes simplex virus type 1. This method is based on a crystal violet uptake of the cells, and the results show a good correlation between the antiviral activity determined by CPE-inhibitory assays and more conventional plaque reduction assay. In addition, also FACS analysis or qRT-PCR have been used by others to evaluate infectivity.[52] However, various infection timings between 24 h and 72 h have been used.[54,55] In addition to the method used, it is valid to consider for how long the infectivity is measured. Measurements after short periods of incubation with the antiviral may show temporarily high inhibition results, which however, may not be relevant anymore after 2 or 3 days of incubation. Here, we set out to explore three well established methods to measure infectivity and also followed the outcome during several days of infection, namely CPE inhibition assay, $TCID_{50}$ assay and confocal microscopy, to evaluate the appearance of newly synthetized viral proteins. We saw some inhibition at first, but only a delay in the infection. This was also verified by an independent assay on cell viability that detects the cellular ATP levels (Figure S6).

Previous studies by others have shown very little effect of Pleconaril on poliovirus 1 (IC_{50} >300 μM) and EV71 (>300 μM).[55] However, better inhibition was suggested to several enterovirus strains including EV5, CVA9, CVB1 and CVB5 (IC_{50} range of 0.001 to 1.05 μM) in CPE assay.[10] Our results with CVA9 and EV1 suggest that despite the preliminary inhibition, virus infection is not really halted; only delayed. Most of the studied derivatives in the previous literature have been proven inactive against CVB3 (IC_{50} >6.1 μM), which is along the lines of our results. Recently more powerful virus inhibitors were developed against HEV71. One of the newest antivirals inhibited the HEV71 CPE with IC_{50} of 25 pM, which is the best recently reported inhibitor.[3]

Conclusions

Our results thus confirm that Pleconaril derivatives (1-4) studied here can be used to label hydrophobic pockets of

enteroviruses EV1 and CVA9. This specified modification of Pleconaril framework combined with gold nanoclusters or fluorescent dye afforded low effectiveness as antivirals without compromising the infectivity of the virus but, instead, provided a new imaging tool for these enteroviruses. Altogether, three different methods verified that our probes bound to the hydrophobic pocket of EV1. TEM showed that only some pockets were easily targeted by the gold probe. This may reflect the normal breathing of the virus and its activity in replacing the present pocket factor by the used probe. We cannot exclude the possibility that some pockets would not be normally empty and act as targets for our probe. The confocal observations of the fluorescent probe **(4)** showed high labeling of the cytoplasmic endosomes, and a high degree of colocalization of the fluorescence probe and the viruses labeled by an independent method by antibodies. The follow up of virus-fluorescence probe conjugate showed decrease of labeling in the endosomes, and a temporary increase of cytoplasmic free labeling of the fluorescent probe **(4)**, demonstrating that, indeed, this probe is dynamic and is able to detach from the virus. Being a hydrophobic dye and a probe, it can freely diffuse through the endosome and other cellular membranes and show a dynamic release probably upon the uncoating event of the virus, or also through a normal exchange of capsid breathing and spontaneous release. **The delay in the dye release and in the viral infection suggests that slight stabilization of the virus due to the probe slows down the uncoating process. This may be taken into account and hopefully helps us to image the virus in live assays with slower kinetics**. The probes developed here thus offer us the opportunity to possibly study the functionality of the pocket in real life, upon real uncoating event.

Acknowledgements

This research is supported by the Academy of Finland (VM: grant 257125, HH: grant 266492) and TEKES FiDiPro project NOVAC. The computational resources were provided by CSC – The Finnish IT Center for Science. We thank J. Koivisto for help with spectroscopic characterization of the probes, M. Pettersson for discussions, and T. J. Sørensen and B. W. Laursen (University of Copenhagen) for providing the azadioxatriangulenium dye.

References

1 T. J. Tuthill, E. Groppelli, J. M. Hogle and D. J. Rowlands, *Curr Top Microbiol Immunol*, 2010, **343**, 43–89.
2 D. Hober and P. Sauter, *Nat. Rev. Endocrinol.*, 2010, **6**, 279–289.
3 L. De Colibus, X. Wang, J. a B. Spyrou, J. Kelly, J. Ren, J. Grimes, G. Puerstinger, N. Stonehouse, T. S. Walter, Z. Hu, J. Wang, X. Li, W. Peng, D. J. Rowlands, E. E. Fry, Z. Rao and D. I. Stuart, *Nat. Struct. Mol. Biol.*, 2014, **21**, 282–8.
4 D. J. Filman, M. W. Wien, J. A. Cunningham, J. M. Bergelson and J. M. Hogle, *Acta Crystallogr. D. Biol. Crystallogr.*, 1998, **54**, 1261–1272.
5 D. J. Filman, R. Syed, M. Chow, A. J. Macadam, P. D. Minor and J. M. Hogle, *EMBO J.*, 1989, **8**, 1567–1579.
6 M. Smyth, T. Pettitt, a. Symonds and J. Martin, *Arch. Virol.*, 2003, **148**, 1225–1233.
7 J. K. Lewis, B. Bothner, T. J. Smith and G. Siuzdak, *Proc. Natl. Acad. Sci. U. S. A.*, 1998, **95**, 6774–6778.
8 M. Oliveira, R. Zhao, W. Lee, M. Kremer, I. Minor, R. Rueckert, G. Diana, D. Pevear, F. Dutko and M. Mckinlay, *Structure*, 1993, **1**, 51–68.
9 M. S. Smyth and J. H. Martin, *Mol. Pathol.*, 2002, **55**, 214–219.
10 D. C. Pevear, T. M. Tull, M. E. Seipel and J. M. Groarke, *Antimicrob. Agents Chemother.*, 1999, **43**, 2109–2115.
11 11G. D. Diana, *Curr. Med. Chem. Anti-Infective Agents*, 2003, **2**, 1–12.
12 S. M. Abdel-Rahman and G. L. Kearns, Antimicrob. Agents Chemother. , 1998, **42**, 2706-2709.
13 M. Oikarinen, S. Tauriainen, S. Oikarinen, T. Honkanen, P. Collin, I. Rantala, M. Mäki, K. Kaukinen and H. Hyöty, *Diabetes*, 2012, **61**, 687–691.
14 P. Kankaanpää, L. Paavolainen, S. Tiitta, M. Karjalainen, J. Päivärinne, J. Nieminen, V. Marjomäki, J. Heino and D. J. White, *Nat. Methods*, 2012, **9**, 683–689.
15 M. Karjalainen, N. Rintanen, M. Lehkonen, K. Kallio, A. Mäki, K. Hellström, V. Siljamäki, P. Upla and V. Marjomäki, *Cell. Microbiol.*, 2011, **13**, 1975–1995.
16 V. Marjomäki, T. Lahtinen, M. Martikainen, J. Koivisto, S. Malola, K. Salorinne, M. Pettersson and H. Häkkinen, *Proc. Natl. Acad. Sci. U. S. A.*, 2014, **111**, 1277–81.
17 J. J. T. Seitsonen, S. Shakeel, P. Susi, A. P. Pandurangan, R. S. Sinkovits, H. Hyvonen, P. Laurinmaki, J. Yla-Pelto, M. Topf, T. Hyypia and S. J. Butcher, *J. Virol.*, 2012, 86, 7207–7215.
18 S. Shakeel, J. J. T. Seitsonen, T. Kajander, P. Laurinmäki, T. Hyypiä, P. Susi and S. J. Butcher, *J. Virol.*, 2013, **87**, 3943–51.
19 G. Abraham and R. J. Colonno, *J. Virol.*, 1984, **51**, 340–345.
20 P. Ruokola, E. Dadu, A. Kazmertsuk, H. Häkkänen, V. Marjomäki and J. a Ihalainen, *J. Virol.*, 2014, **88**, 8504–13.
21 M. Schmidtke, U. Schnittler, B. Jahn, H. Dahse and a Stelzner, *J. Virol. Methods*, 2001, **95**, 133–143.
22 J. Z. Porterfield and A. Zlotnick, *Virology*, 2010, **407**, 281–288.
23 T. S. Walter, J. Ren, T. J. Tuthill, D. J. Rowlands, D. I. Stuart and E. E. Fry, *J. Virol. Methods*, 2012, **185**, 166–170.
24 V. Marjomäki, V. Pietiäinen, H. Matilainen, P. Upla, J. Ivaska, L. Nissinen, H. Reunanen, P. Huttunen, T. Hyypiä and J. Heino, *J. Virol.*, 2002, **76**, 1856–1865.
25 A. M. De Palma, I. Vliegen, E. De Clercq and J. Neyts, *Med. Res. Rev.*, 2008, **28**, 823–884.
26 26N. Reisdorph, J. J. Thomas, U. Katpally, E. Chase, K. Harris, G. Siuzdak and T. J. Smith, *Virology*, 2003, **314**, 34–44.
27 V. L. Giranda, G. R. Russo, P. J. Felock, T. R. Bailey, T. Draper, D. J. Aldous, J. Guiles, F. J. Dutko, G. D. Diana, D. C. Pevear and M. McMillan, *Acta Crystallogr. D. Biol. Crystallogr.*, 1995, **51**, 496–503.
28 Y. Zhang, A. a Simpson, R. M. Ledford, C. M. Bator, S. Chakravarty, G. a Skochko, T. M. Demenczuk, A. Watanyar, D. C. Pevear and M. G. Rossmann, *J. Virol.*, 2004, **78**, 11061–11069.
29 H. J. Thibaut, A. M. De Palma and J. Neyts, *Biochem. Pharmacol.*, 2012, **83**, 185–192.
30 K. Salorinne, T. Lahtinen, V. Marjomäki and H. Häkkinen, *CrystEngComm*, 2014, **16**, 9001–9009.
31 P. D. Jadzinsky, G. Calero, C. J. Ackerson, D. A. Bushnell and R. D. Kornberg, *Science*, 2007, **318**, 430–433.
32 K. Salorinne, T. Lahtinen, S. Malola, J. Koivisto and H. Häkkinen, *Nanoscale*, 2014, **6**, 7823–6.
33 T. J. Sørensen, E. Thyrhaug, M. Szabelski, R. Luchowski, I. Gryczynski, Z. Gryczynski and B. W. Laursen, *Methods Appl. Fluoresc.*, 2013, **1**, 25001.

34 E. Thyrhaug, T. J. Sørensen, I. Gryczynski, Z. Gryczynski and B. W. Laursen, *J. Phys. Chem. A*, 2013, **117**, 2160–2168.
35 35S. K. Tsang, P. Danthi, M. Chow and J. M. Hogle, *J. Mol. Biol.*, 2000, **296**, 335–340.
36 A. J. Benie, R. Moser, E. Bäuml, D. Blaas and T. Peters, *J. Am. Chem. Soc.*, 2003, **125**, 14–15.
37 A. Bhunia, S. Bhattacharjya and S. Chatterjee, *Drug Discov. Today*, 2012, **17**, 505–513.
38 C. Rademacher and T. Peters, *Top. Curr. Chem.*, 2008, **273**, 183–202.
39 M. Huttunen, M. Waris, R. Kajander, T. Hyypiä and V. Marjomäki, *J. Virol.*, 2014, **88**, 5138–51.
40 P. Upla, V. Marjomäki, L. Nissinen, C. Nylund, M. Waris, T. Hyypiä and J. Heino, *J. Virol.*, 2008, **82**, 1581–1590.
41 J. D. Yoder, J. O. Cifuente, J. Pan, J. M. Bergelson and S. Hafenstein, *J. Virol.*, 2012, **86**, 12571–12581.
42 A. M. Macleod, D. R. Mitchell, N. J. Palmer, H. Van De Poël, K. Conrath, M. Andrews, P. Leyssen and J. Neyts, *ACS Med. Chem. Lett.*, 2013, **4**, 585–589.
43 M. Schmidtke, P. Wutzler, R. Zieger, O. B. Riabova and V. A. Makarov, *Antiviral Res.*, 2009, **81**, 56–63.
44 N. Ismail-Cassim, C. Chezzi and J. F. E. Newman, *J. Gen. Virol.*, 1990, **71**, 2283–2289.
45 Q. Li, a G. Yafal, Y. M. Lee, J. Hogle and M. Chow, *J. Virol.*, 1994, **68**, 3965–3970.
46 U. Katpally, T.-M. Fu, D. C. Freed, D. R. Casimiro and T. J. Smith, *J. Virol.*, 2009, **83**, 7040–7048.
47 M. A. Jiménez-Clavero, A. Douglas, T. Lavery, J. A. Garcia-Ranea and V. Ley, *Virology*, 2000, **270**, 76–83.
48 B. Bothner, X. F. Dong, L. Bibbs, J. E. Johnson and G. Siuzdak, *J Biol Chem*, 1998, **273**, 673–676.
49 B. Bothner, D. Taylor, B. Jun, K. K. Lee, G. Siuzdak, C. P. Schlutz and J. E. Johnson, *Virology*, 2005, **334**, 17–27.
50 Roy and C. B. Post, *Proc. Natl. Acad. Sci.*, 2012, **109**, 5271–5276.
51 Y. Liu, J. Sheng, a. Fokine, G. Meng, W.-H. Shin, F. Long, R. J. Kuhn, D. Kihara and M. G. Rossmann, *Science* , 2015, **347**, 71–74.
52 P. Plevka, R. Perera, M. L. Yap, J. Cardosa, R. J. Kuhn and M. G. Rossmann, *Proc. Natl. Acad. Sci. U. S. A.*, 2013, **110**, 5463–7.
53 V. Rincón, A. Rodríguez-Huete, S. López-Argüello, B. Ibarra-Molero, J. M. Sanchez-Ruiz, M. M. Harmsen and M. G. Mateu, *Structure*, 2014, **22**, 1560–1570.
54 V. a. Makarov, O. B. Riabova, V. G. Granik, P. Wutzler and M. Schmidtke, *J. Antimicrob. Chemother.*, 2005, **55**, 483–488.
55 H. J. Thibaut, P. Leyssen, G. Puerstinger, A. Muigg, J. Neyts and A. M. De Palma, *Antiviral Res.*, 2011, **90**, 213–217.